

## Structure–Activity Relationships in a Series of Bisquaternary Bisphthalimidine Derivatives Modulating the Muscarinic M<sub>2</sub>-Receptor Allosterically

Hector M. Botero Cid, Christian Tränkle,<sup>†</sup> Knut Baumann, Rainer Pick, Elisabeth Mies-Klomfass,<sup>†</sup> Evi Kostenis,<sup>†</sup> Klaus Mohr,<sup>†</sup> and Ulrike Holzgrabe\*

Pharmaceutical Chemistry, Institute of Pharmacy, University of Würzburg, Am Hubland, 97074 Würzburg, FRG, and Pharmacology and Toxicology, Institute of Pharmacy, University of Bonn, An der Immenburg 4, 53121 Bonn, FRG

Received December 2, 1999

Hexane-bisammonium-type compounds containing lateral phthalimide moieties are well-established ligands of the common allosteric binding site of muscarinic M<sub>2</sub> receptors. Previous structure–activity relationships (SAR) revealed two positively charged centers and two lateral phthalimide moieties in a defined arrangement to be essential of a high allosteric potency. The purpose of this study was to replace one carbonyl group of the phthalimides with hydrogens, hydroxy, alkoxy, phenyl, benzyl, and benzylidene groups in order to check the influence of these substituents on the allosteric activity in antagonist-linked receptors. The analysis of the quantitative SAR indicated that a high allosteric potency is related to a certain amount of rigidity as well as polarizability and the ability to form hydrophobic interactions.

### Introduction

Several bisquaternary compounds belonging to different pharmacological groups are known to retard the dissociation of antagonists, such as *N*-methylscopolamine (NMS), from the muscarinic acetylcholine receptor.<sup>1,2</sup> This effect, being indicative of an allosteric modulation of the antagonist receptor complex, is caused by the binding of an allosteric modulator in a receptor whose orthosteric site is occupied by the antagonist.<sup>3,4</sup> The comparison of the allosteric modulators alcuronium,<sup>5</sup> tubocurarine,<sup>6</sup> gallamine,<sup>7</sup> and W84<sup>8</sup> (a bisphthalimide compound derived from hexamethonium), utilizing the Kohonen neural network, revealed the dependence of the allosteric potency on the molecular electrostatic potential (MEP) as well as steric parameters.<sup>9</sup> To elucidate the binding mode a 3D quantitative structure–activity analysis was subsequently performed in an extended series of structurally diverse compounds of different allosteric potency.<sup>10</sup> Using the features of a molecular shape analysis, alcuronium was taken as a template molecule for comparison of W84-derivatives and several bispyridinium-derived compounds (i.e. WDUO, DUO–O, IWDUO). The pharmacophoric elements turned out to be two positively charged nitrogens and two aromatic areas arranged in a sandwich-like geometry. The biological activity within this extended series was found to be related to the nonoverlap volume and the MEP, described as integrated potential field differences. These findings supported the hypothesis that the allosteric binding site seems to have space for voluminous substituents especially on the lateral heterocycle moieties of the bisquaternary molecules.<sup>11</sup> The purpose of this study is to check the influence of the size, lipophilicity, and electronic properties of substituents in position 3 of the phthalimide. In a preceding step the aromatic lateral heterocycles of the lead

compound W84 were replaced with corresponding saturated skeletons.<sup>12</sup> This structural change resulted in a decrease of allosteric potency. Reduction in size decreases the potency by a factor of 400. Thus, we decided to keep the main part of the aromatic phthalimide ring but to replace, on one hand, one carbonyl functional group with two hydrogens as well as hydroxy and alkoxy groups and with benzyl and phenyl substituents. On the other hand, different benzylidene isomers (*E* and *Z*) of the phthalimide skeleton were synthesized in order to investigate the possible stereoselectivity of the allosteric modulation. Finally, an analysis of quantitative structure–activity relationships (QSAR) was performed in order to explain the potency of the newly synthesized compound and to further characterize the allosteric binding site.

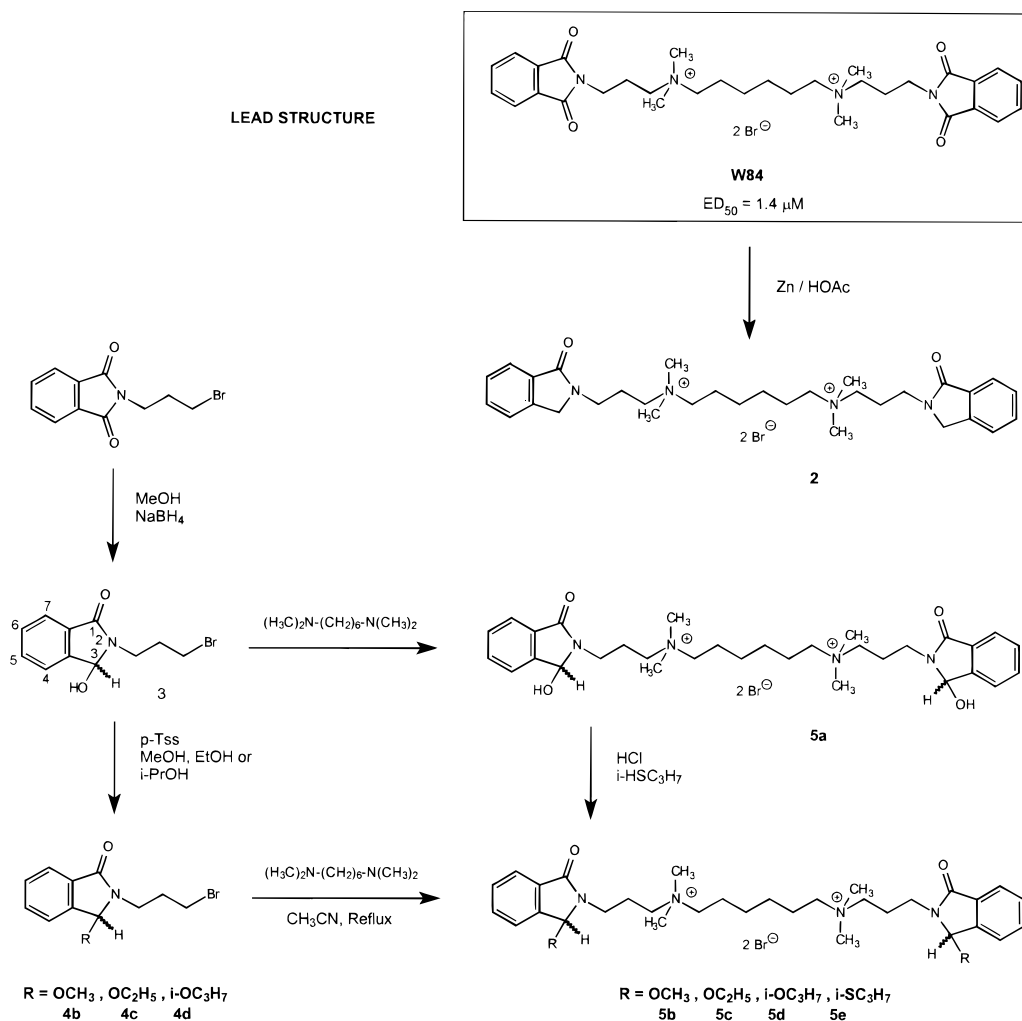
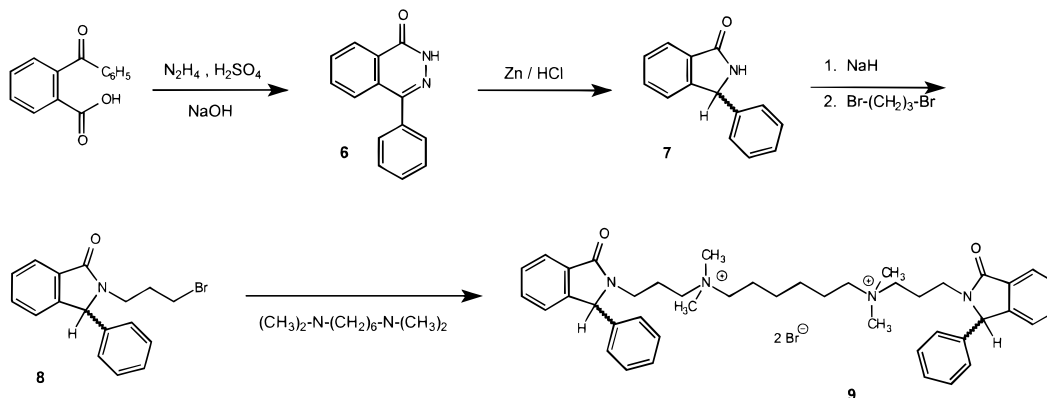
### Chemistry

**Synthesis.** The synthesis of the phthalimidine derivative **2** started off from the lead compound W84<sup>13</sup> (Scheme 1). Reduction using Zn powder in glacial acetic acid and 10% propionic acid gave the methylene compound **2** in a rather good yield. The synthesis of the alkoxyphthalimidines started off from *N*-bromopropylphthalimide. Selective reduction of one of the two carbonyl functions was achieved by means of sodium borohydride in methanol. The hydroxy group of the obtained **3** was replaced with the appropriate alkoxy groups by a nucleophilic substitution using the corresponding alcohols.<sup>14</sup> Then the exhaustive alkylation of *N*<sup>1</sup>,*N*<sup>1</sup>,*N*<sup>6</sup>,*N*<sup>6</sup>-tetramethyl-1,6-hexanediamine with two molecules of **4b–d** gave the bisquaternary compounds **5b–d** by refluxing for 5–24 h in a polar solvent. The corresponding hydroxy compound **5a** was achieved by heating 2 mol of **3** with 1 mol of the bisamine in acetone. The hydroxy groups in **5a** were replaced with isopropylmercapto groups by refluxing in propanethiolo under acidic conditions to give **5e**.

The introduction of a phenyl or methyl group into position 3 of the phthalimide skeleton (Scheme 2) was

\* Corresponding author. Tel: 0931/8885460. Fax: 0931/8885494. E-mail: holzgrab@pharmazie.uni-wuerzburg.de.

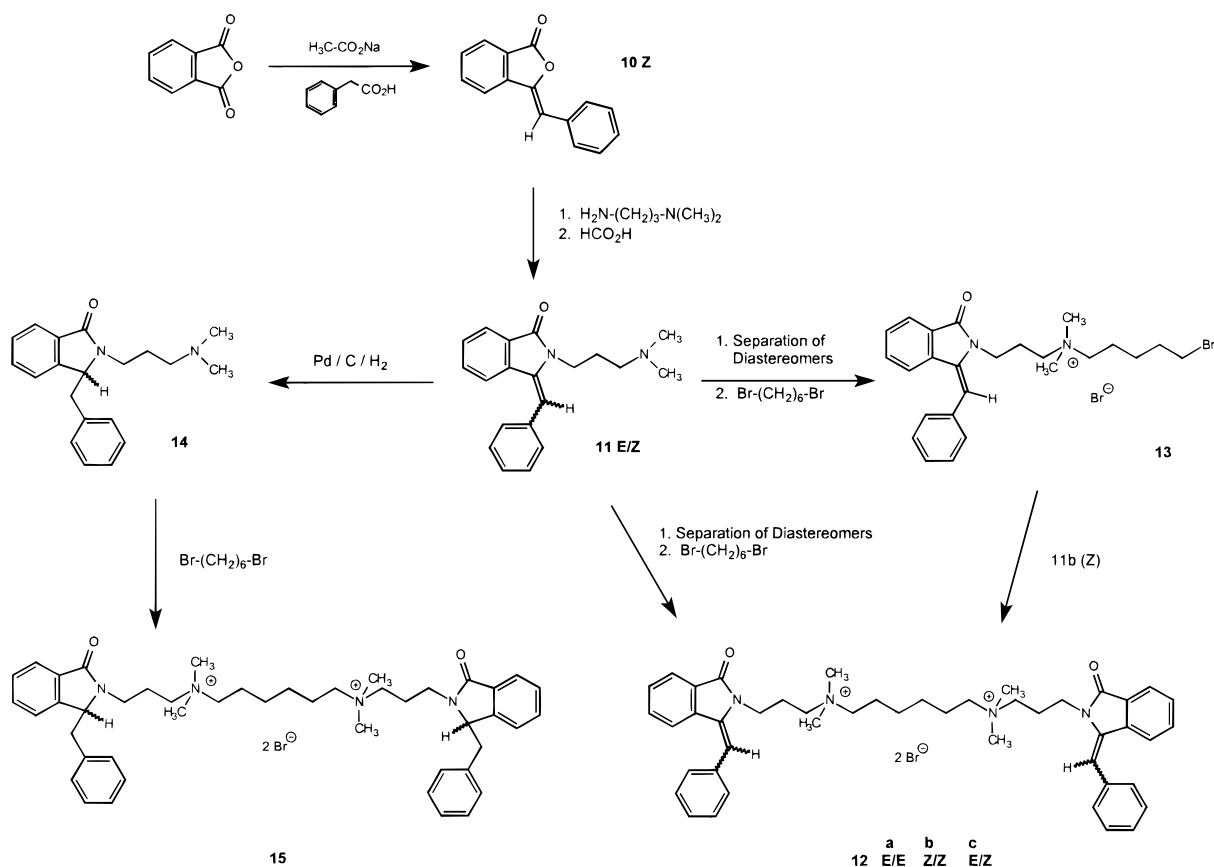
<sup>†</sup> University of Bonn.

**Scheme 1.** Synthesis Pathway of the Compounds **5****Scheme 2.** Synthesis Pathway of the Compound **9**

achieved by partially utilizing the synthesis pathway described by Gabriel and Naumann.<sup>15</sup> *o*-Benzoylbenzoic acid was converted to phenylphthalazone **6** using hydrazine sulfate in sodium hydroxide solution. Subsequent reduction with Zn powder in hydrochloric acid gave the 3-phenylphthalimidine **7**, which was N-alkylated with 1,3-dibromopropane in the presence of sodium hydride in tetrahydrofuran to achieve **8**. It was impossible to obtain the corresponding methyl derivative because only a mixture of many products could be isolated from the reaction solution. Two molecules of **8**

were connected with *N*<sup>1</sup>,*N*<sup>1</sup>,*N*<sup>6</sup>,*N*<sup>6</sup>-tetramethyl-1,6-hexanediamine by refluxing in acetonitrile to give **9**.

To obtain the benzylidene and benzyl phthalimidine derivatives **12** and **15**, respectively, phthalic anhydride, phenylacetic acid, and sodium acetate were heated to 250–300 °C to give the *Z* isomer of 3-benzylphthalide **10** (Scheme 3).<sup>16</sup> The oxygen of the phthalide was replaced with a nitrogen by refluxing with dimethylaminopropylamine and subsequent dehydration using formic acid. The so obtained **11** is a mixture of about 90% *E* and 10% *Z* isomer which was separated by means

**Scheme 3.** Synthesis Pathway of the Compounds **12** and **15**

of column chromatography. Each isomer was converted to the corresponding bisquaternary benzylidene compounds **12a,b** (*E/E*, *Z/Z*) with 1,6-dibromohexane. In case of the *E/Z* isomer **12c**, the *E* benzylidene phthalimidopropylamine was selectively alkylated with 1,6-dibromohexane to give **13**. At last, the *Z*-isomer is connected to the opposite end of the hexamethonium middle chain. For the benzyl derivative **15** the mixture of isomers of **11** was hydrogenated with  $\text{Pd/C/H}_2$ . Two molecules of **14** were connected with 1,6-dibromohexane.

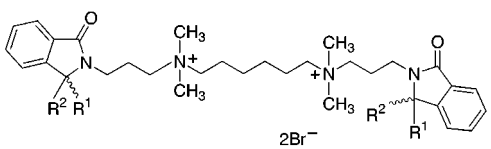
**Stereochemistry.** Since the reduction of bromopropylphthalimide created a center of chirality ( $\rightarrow$ **3**; Scheme 1), it is expected that the last step of the synthesis pathway will result in a mixture of two enantiomers and a meso isomer (**5a–e**). We tried to find out the ratio of the isomers by means of chiral column chromatography and NMR spectroscopy (see Table 5, Experimental Section).

The  $^1\text{H}$  and  $^{13}\text{C}$  NMR of all chiral compounds does neither in  $\text{CDCl}_3$  nor in  $\text{DMSO}-d_6$  show two sets of signals corresponding to the racemate and the diastereomeric meso-compound. Additionally, neither with chiral shift reagents, such as  $\text{Eu}(\text{tfc})_3$ , nor with different cyclodextrin derivatives could two or three sets of signals be detected (although a complexation was observed in either case). Column chromatography using a chiral stationary phase, polymer phenylethylacrylamide, which has already been successfully applied in a similar case,<sup>11</sup> shows only one broad peak. Similar results were obtained with cyclodextrin-modified capillary electrophoresis. Since there was no evidence of diastereomers in either method, it may be assumed that either the racemic mixture or the meso isomer was

formed. The defined melting points measured in each case may further support this hypothesis. Because the compounds **5** did not exhibit a higher potency than the lead compound W84 (see below) and, due to N,O-acetal function, the center of chirality is supposed to be stereochemically unstable, a separation of the isomers was not performed.

Accordingly, for the phenyl-substituted compound **9** only one set of signals could be detected in the NMR spectra. Interestingly, the signals for the hydrogens next to the imide nitrogens are very separated (3.32 versus 3.74 ppm; see Table 1). This is caused by the phenyl ring in position 3, which is orientated to the bisquaternary middle chain, and in line with that, one of the  $\text{N}_{\text{Phth}}$ -methylene hydrogens is influenced by the ring current effect resulting in a shielding of the hydrogen. The same was found to be true for the benzyl derivative **15**.

The configuration of the isomers of **12** was determined by means of NOE experiments. Saturation of the signal of the methine proton in **12a** resulted in an enhancement of the  $\text{N}_{\text{Phth}}\text{-CH}_2\text{CH}_2$  signals and vice versa, which indicates a spatial neighborhood of these groups, and thus an *E*-configuration. Additionally, the signals of the propylene chain, the *N*-methyl group, and partly the hexane chain of the *Z*-isomer (**12b**) are upfield shifted in comparison with the signals of the *E*-isomer (**12a**). The shielding is found to be most pronounced for the  $\text{N}_{\text{Phth}}\text{CH}_2\text{CH}_2\text{CH}_2\text{N}^{+-}$  ( $\Delta\delta = 0.6\text{--}0.7$  ppm). In turn, the aromatic hydrogen next to the benzylidene group are upfield shifted in case of the *E*-isomer (**12a**) in comparison with the *Z*-isomer. These effects are caused by the shielding ring current effect of the phenyl ring, which

**Table 1.** Substituents and  $\log(1/EC_{50})$  of the Compounds Studied<sup>a</sup>


compd	R <sup>1</sup> , R <sup>2</sup>	$\log(1/EC_{50}) \pm SEM$	surf (Å <sup>2</sup> )	vol (Å <sup>3</sup> )	$\log P$	MR (Å <sup>3</sup> )	pol (Å <sup>3</sup> )	dip (D)	ind	222
W84	=O, -	5.85 ± 0.05	274.15	489.12	1.46	43.51	13.38	2.878	1	13
<b>2</b>	H, H	5.70 ± 0.18	276.71	490.96	1.55	43.39	12.80	3.729	0	9
<b>5a</b>	OH, H	5.22 ± 0.15	271.40	506.08	1.45	44.42	13.28	3.167	0	9
<b>5b</b>	OCH <sub>3</sub> , H	5.17 ± 0.35	310.47	554.78	1.72	49.17	14.78	3.840	0	9
<b>5c</b>	OC <sub>2</sub> H <sub>5</sub> , H	5.64 ± 0.11	340.02	611.20	2.07	53.91	16.07	3.932	0	9
<b>5d</b>	O- <i>i</i> -C <sub>3</sub> H <sub>7</sub> , H	5.80 ± 0.47	354.39	639.61	2.48	58.33	17.32	3.675	0	9
<b>5e</b>	S- <i>i</i> -C <sub>3</sub> H <sub>7</sub> , H	5.90 ± 0.67	376.16	663.70	2.92	64.51	19.18	4.174	0	9
<b>9</b>	C <sub>6</sub> H <sub>5</sub> , H	6.10 ± 0.04	313.26	677.27	3.40	67.67	20.60	3.779	0	16
<b>12a</b> ( <i>E/E</i> )	=CH-C <sub>6</sub> H <sub>5</sub> , -	7.15 ± 0.07	342.99	713.02	2.96	73.81	23.97	3.194	1	22
<b>12b</b> ( <i>Z/Z</i> )	=CH-C <sub>6</sub> H <sub>5</sub> , -	7.07 ± 0.05	341.34	709.35	2.96	73.81	24.58	3.040	1	22
<b>12c</b> ( <i>Z/E</i> )	=CH-C <sub>6</sub> H <sub>5</sub> , -	7.18 ± 0.02	342.17	711.19	2.96	73.81	24.28	3.117	1	22
<b>15</b>	CH <sub>2</sub> -C <sub>6</sub> H <sub>5</sub> , H	6.00 ± 0.04	353.88	739.08	3.65	72.42	21.87	3.746	0	15

<sup>a</sup> Symbols: surf., surface; vol, volume;  $\log P$ , octanol/water partition coefficient; MR, molar refractivity; pol, mean  $\alpha$ -polarizability (MOPAC); dip, dipole moment (MOPAC); ind, indicator variable for a double bond in position 3; 222, count of  $sp^2-sp^2$  substructures (cf. text).

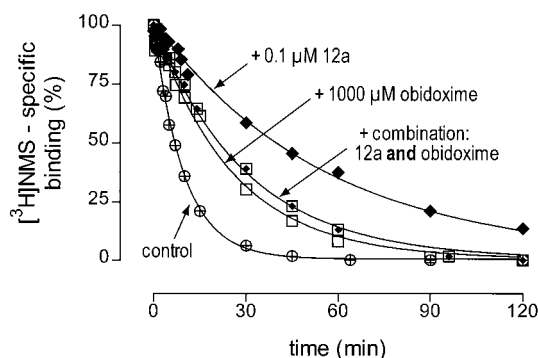


**Figure 1.** [<sup>3</sup>H]NMS dissociation from muscarinic M<sub>2</sub> receptors under control conditions and in the presence of the indicated test compounds in Na,K,P<sub>i</sub> buffer. Note that obidoxime attenuates the allosteric action of **12a**. Shown is a representative set of experiments. Monoexponential curve fitting.

is orientated either to the hexamethonium chain (*Z*) or to the phthalimidine ring (*E*). Similar results were reported by Marsili et al.<sup>17</sup> for corresponding benzylidene-nephthalimidines.

**Pharmacology.** The ability of the compounds to retard the dissociation of the radioligand [<sup>3</sup>H]*N*-methylscopolamine ([<sup>3</sup>H]NMS) was measured in porcine cardiac M<sub>2</sub> receptors. All compounds reduced the apparent rate constant of [<sup>3</sup>H]NMS dissociation  $k_{-1}$  concentration-dependently. The concentration of a test compound inducing a reduction of  $k_{-1}$  to 50% of the control value ( $EC_{50}$ ) served as a measure of the allosteric effect (Table 1). At the  $EC_{50}$  concentration, occupancy of the NMS-receptor complexes by the allosteric agent can be considered as half-maximal. In this case, the  $EC_{50}$  value is equivalent to the  $K_D$  value of allosteric binding.<sup>4</sup> To check the topology of binding, the most potent compound (**12a**) was tested to determine whether the allosteric retardation of [<sup>3</sup>H]NMS dissociation was sensitive toward the "allosteric antagonist" obidoxime. The experimental design is illustrated in Figure 1.

## Results and Discussion

The allosteric potency of the phthalimidine derivatives **2**, **5a–e**, **9**, and **15** is found to be on the same order

of magnitude as the lead compound W84. Almost all alkoxy compounds **5** are less active than W84. At a first glance, within this series the potency seems to increase with the increasing size of the substituents. However, the phenyl- and benzyl-substituted compounds **9** and **15**, respectively, exhibit the same potency as W84. But even more interesting, the introduction of a double bond in position 3, which makes the lateral moiety more rigid, enhances the potency by more than 1 order of magnitude. To quantitatively explain the differences in the allosteric potency of the compounds, studied herein, a QSAR analysis was performed. Table 1 shows the compounds under scrutiny, their corresponding potencies, and molecular descriptors.

Since, in previous studies, the allosteric potency was found to depend on the steric bulk and on the lipophilicity, parameters were considered which characterize these properties, e.g. the STERIMOL parameters  $L$ ,  $B_1$ , and  $B_5$  as well as MR (molar refractivity) and  $\pi$ . Unfortunately, these parameters could not be found for all substituents in the literature.<sup>18–20</sup> To apply comparable parameters, they were computed using the HyperChem/ChemPlus package (see the methods). As a model, corresponding *N*-methylphthalimide moieties were built up using the model builder and the MM+ program. Next, the octanol/water partition coefficient ( $\log P$ ), the steric parameters, volume and surface area, as well as polarizability and refractivity, which is a function of steric bulk and polarizability, were calculated. Moreover, an indicator variable which takes a value of 1 if there is a double bond in position 3 and a zero otherwise was added to the set of descriptors. This indicator variable accounts for the altered rigidity of the lateral moiety. After an initial screening of the descriptors it turned out that polarizability and the indicator variable were the most important descriptors. To improve the QSAR models we recalculated the polarizability of the substituents on a higher level of sophistication using MOPAC<sup>21</sup> and replaced HyperChem's estimate of the polarizability by MOPAC's mean  $\alpha$ -polarizability.<sup>22</sup> The MOPAC calculation also yielded the dipole moment of the substituents, which was also included in the analysis. Furthermore, we added a



**Table 2.** Correlation Matrix of the Final Set of Descriptors<sup>a</sup>

no.	variable	log(1/EC <sub>50</sub> )	surf	vol	log <i>P</i>	MR	pol	dip	ind
1	surf	0.432							
2	vol	0.707	0.837						
3	log <i>P</i>	0.611	0.747	<b>0.952</b>					
4	MR	0.806	0.759	<b>0.982</b>	<b>0.938</b>				
5	pol	0.877	0.691	<b>0.946</b>	<b>0.877</b>	<b>0.987</b>			
6	dip	-0.478	0.396	0.084	0.172	-0.044	-0.179		
7	ind	0.787	0.009	0.240	0.113	0.371	0.498	-0.822	
8	222	0.939	0.264	0.668	0.596	0.778	0.859	-0.591	0.800

<sup>a</sup> The cluster of highly intercorrelated descriptors is set in bold letters.

**Table 3.** Best One- and Two-Parameter QSAR Models, Ranked According to  $Q^2$ <sup>a</sup>

no.	$x_1$	$x_2$	$s_{PRESS}$	$Q^2$	$s$	$R^2$	$p_{rand}(Q^2)$	$p_{rand}(R^2)$	$\beta_0$	$\beta_1$	$\beta_2$
1	ind	pol	0.285	0.865	0.202	0.932	0.0002	0.0002	3.988	0.664	0.100
2	222	surf	0.286	0.864	0.222	0.918	0.0012	0.0002	3.265	0.111	0.004
3	ind	MR	0.311	0.839	0.211	0.926	0.0002	0.0002	3.814	0.807	0.033
4	222		0.296	0.838	0.253	0.882	0.0028	<0.0002	4.462	0.117	
5	pol	dip	0.363	0.781	0.273	0.876	0.0032	0.0002	5.672	0.127	-0.557
6	ind	vol	0.364	0.780	0.239	0.905	0.0026	0.0002	3.165	0.933	0.004
7	ind	log <i>P</i>	0.376	0.762	0.250	0.896	0.0042	<0.0002	4.558	1.036	0.471

<sup>a</sup> Symbols:  $x_i$ , variables included in the model; the numbering scheme follows the one given in Table 2;  $s_{PRESS}$ , cross-validated standard deviation (the square root of PRESS (predicted error sum of squares) divided by the degrees of freedom);  $Q^2$ , cross-validated coefficient of determination;  $s$ , standard deviation (the square root of the residual sum of squares divided by the degrees of freedom);  $R^2$ , coefficient of determination;  $p_{rand}(Q^2)$ , probability that a scrambled response vector yields a higher  $Q^2$  than the original one;  $p_{rand}(R^2)$ , same as  $p_{rand}(Q^2)$  for  $R^2$ ;  $\beta_i$ , regression coefficient for the  $i$ th variable;  $\beta_0$ , intercept. All reported regression coefficients are significant ( $t$ -test,  $\alpha = 0.1$ , two-sided).

particular SE-descriptor,<sup>23,24</sup> referred to as  $sp^2-2-sp^2$  (abbr, 222), expected to characterize the rigidity of the substituents even more thoroughly. The 222-descriptor counts the number of unique substructural fragments that start on a  $sp^2$ -hybridized atom and end on a  $sp^2$ -hybridized atom separated by two bonds (e.g.  $H_2C=CH-CH=CH_2 \rightarrow 222 = 2$ ). This descriptor can also be viewed as a special atom pair.<sup>25</sup> In this series of molecules it characterizes, among other things, the overall rigidity of the substituent, rather than just the hybridization in position 3 like the indicator variable. Moreover, it does not only characterize the number of double bonds but also the arrangement of double bonds in the molecule. A correlation matrix of the final set of descriptors plus log(1/EC<sub>50</sub>) is shown in Table 2. The correlation matrix deserves some comments: First, the single variable correlation between 222 and log(1/EC<sub>50</sub>) is very good. The corresponding regression model yields a coefficient of determination ( $R^2$ ) of 0.882 and a cross-validated coefficient of determination ( $Q^2$ ) of 0.838 and is by far the best one parameter regression model that can be built for the data set with this set of descriptors. Second, there is a cluster of four descriptors, namely, volume, log *P*, refractivity, and polarizability, that are highly intercorrelated ( $r > 0.87$ ). There was no substituent in this series that breaks this correlation. For hydrophobic substituents it is known that there exists a close interrelation between volume, surface, refractivity, and lipophilicity.<sup>26</sup> As a consequence, we anticipate that it will be difficult to distinguish the effect of one of these descriptors from the others.

Since the object-to-variable ratio is rather low (12/7) only a subset of the descriptors given above should be used to derive a QSAR. Since all one-parameter regression models apart from the aforementioned one are unsatisfactory with respect to  $Q^2$  ( $Q^2 < 0.5$ ), we computed all two-parameter regression models. In Table 3 all two-parameter models with  $Q^2$  values larger than 0.7 and descriptor pairs correlated less than 0.5 ( $r <$

0.5) are shown. Additionally, the best one-parameter regression model is also given. All regression models given in Table 3 were computed with the entire set of structures ( $n = 12$ ). The statistical parameters of the equations are good, and particularly, the internal predictive power ( $Q^2$ ,  $s_{PRESS}$ ) of the models is high ( $Q^2 > 0.76$ ). Nonetheless, it must be noted that all models including the indicator variable predict (cross-validation) either compound W84 or compound **2** substantially worse than the remaining compounds. Note also that the high  $R^2$  and  $Q^2$  values indicate better models than they actually are.  $R^2$  and  $Q^2$  are slightly inflated because the data set is clustered into few highly potent and many less potent compounds. Plots of the experimental versus the predicted activities for the best two models are included in the Supporting Information.

Variable selection may be prone to chance correlation. Topliss and Edwards<sup>27</sup> showed that screening a large number of variables which in fact were not related to the response (since they were random numbers) often resulted in satisfactory regression equations. In this study, the probability of chance correlation was reduced by selecting variables that maximized  $Q^2$  rather than selecting variables that maximized  $R^2$ . Put another way, the predictive power of the models was optimized and not the fit. Nevertheless, to thoroughly assess the probability that the reported models may have been generated just by chance we also ran a permutation test.<sup>27,28</sup> The employed permutation test is based on the repetitive randomization of the response vector. In each cycle of the test the response vector is randomly rearranged, the regression is carried out on the scrambled data, and  $Q^2$  and  $R^2$  values are recorded for each cycle. If the majority of  $Q^2$  and  $R^2$  values of the scrambled data sets is much lower than the  $Q^2$  and  $R^2$  of the original data set it can be concluded that the derived model is relevant. The number of permutations for each test was 5000. The probability that a scrambled response vector yields a larger  $Q^2$  or  $R^2$  value than the original vector

is recorded in the variables  $p_{\text{rand}}(Q^2)$  and  $p_{\text{rand}}(R^2)$  of Table 3. If a scrambled vector gave rise to a larger  $Q^2$  and  $R^2$  value, the correlation between the scrambled vector and the original one was generally rather high. Hence, the probability that the reported models may have been generated just by chance is low.

What do we learn from the QSAR models about the structural requirements for allosteric potency? First of all, it is worth noting that each model contains a descriptor characterizing rigidity (Ind or 222). Even the 222-descriptor alone yields a good model. Thus, we hypothesize that a certain amount of rigidity of the lateral substituent is important for allosteric potency. The fact that rigidity is important can most easily be seen by comparing the potency of the benzylidene-substituted compounds **12** to the benzyl-substituted compound **15**. Compound **15** was found to be 1 order of magnitude less potent than compounds **12**. Since the most striking difference between both compounds is the higher rigidity of **12** created by the double bond, it is likely that the higher affinity of **12** is caused by a smaller loss of conformational entropy<sup>29</sup> on binding to the receptor molecule.

Second, in the case of the indicator variable, good models are obtained if it is combined with polarizability, molar refraction, volume, or  $\log P$ . This was actually within expectation, since these parameters are highly intercorrelated. Thus, we expect that all four parameters in combination with the indicator variable encode one underlying phenomenon. Whether, the set of parameters encodes the substituents' ability to interact with the target receptor via van der Waals forces (polarizability, molar refraction) or via hydrophobic interactions ( $\log P$ ) cannot be determined unequivocally from these models. High polarizability is usually advantageous for induction forces (permanent dipole-induced dipole) or dispersion forces (instantaneous dipole-induced dipole), whereas substituents with a high  $\log P$  value are likely to exhibit hydrophobic interactions.<sup>29,30</sup> Model 6, which uses polarizability and dipole moment as explanatory variables can, however, shed some light on the interaction forces. Since dipole moment enters the respective regression equation with a negative sign, more polar molecules are less potent according to this equation. Thus, it is more likely that nonpolar interactions (dispersion forces) and hydrophobic interactions drive the binding process rather than inductive interactions. The latter type of interaction would require high polarizability and high dipole moment.

Compounds **12** appears to have a 20-fold higher affinity for NMS-occupied receptors than the parent compound W84. Previously, it was shown that structurally closely related compounds may reveal a divergent mode of allosteric action.<sup>3</sup> In view of the large size of the benzylidene moieties, we aimed to check whether **12a** still utilizes the common allosteric site.<sup>31</sup> Therefore, it was tested whether the allosteric action of **12a** is sensitive toward the "allosteric antagonist" obidoxime (Figure 2a,b).<sup>3</sup> Obidoxime interfered with the action of **12a** in a competitive fashion. The equilibrium dissociation constant of obidoxime binding derived from the experiments amounted to  $pK_B = 4.34 \pm 0.52$ ,  $n = 4$  (mean  $\pm$  SEM). When the action of W84, which is one

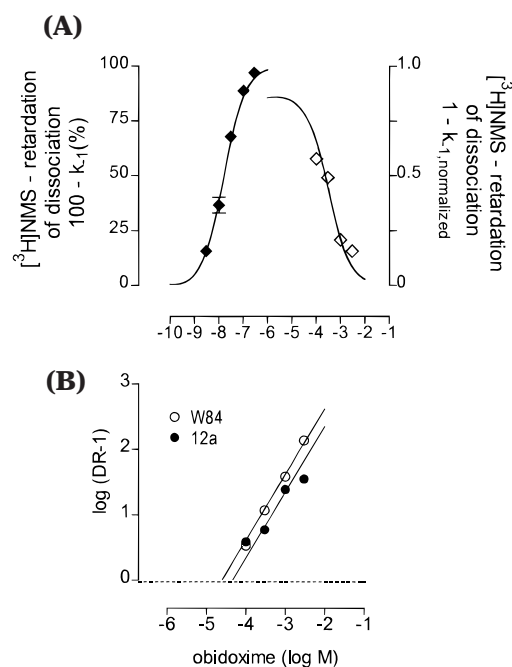
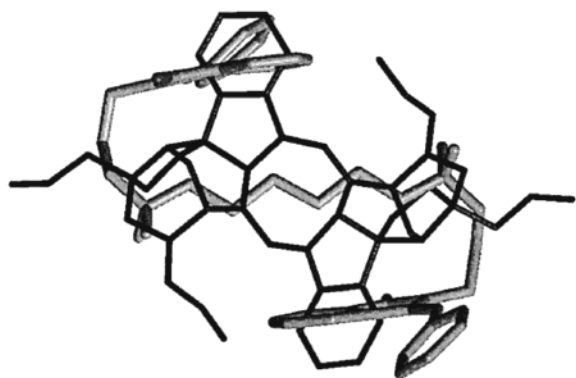


**Figure 2.** (a) Obidoxime-induced attenuation (open diamonds, right ordinate) of the effect of **12a** (0.1  $\mu$ M, filled diamonds, left ordinate) on [<sup>3</sup>H]NMS dissociation. Left ordinate: The effect of **12a** alone (filled diamonds) is expressed as percentage of the maximum possible effect, i.e.,  $k_{-1} = 0$ . Right ordinate: Effect of 0.1  $\mu$ M **12a** in the presence of increasing concentrations of obidoxime; the respective  $k_{-1}$  in the presence of obidoxime alone was set to  $k_{-1, \text{normalized}} = 1.0$ . Simultaneous curve fitting according to ref 28. (b) Schild plot for **12a**; dose ratios  $DR = EC_{0.5, \text{obidoxime}}/EC_{0.5, \text{control}}$  and the line were derived from Figure 4A. W84 data were taken from ref 3.

of the prototype allosteric agents using the common allosteric site of  $M_2$  receptors was antagonized by obidoxime, a similar  $pK_B = 4.61 \pm 0.05$ ,  $n = 5$ , was found. The equal sensitivity of **12a** and W84 against obidoxime suggests that **12a** acts at the same site as W84 does, i.e., the common allosteric site.

Since the geometric isomers of the benzylidene-substituted compound **12**, the *EE*, the *ZZ*, and the *EZ*-isomer, exhibit the same allosteric potency, the interaction of these groups with the receptor is not stereoselective. As can clearly be seen in Figure 3, in these compounds the phenyl rings in position 3 are pointing to different directions in space when adopting the pharmacophoric conformation described in the Introduction. On the other hand, it is conceivable that the benzylidene system instead of the phthalimide occupies the aromatic area of the pharmacophore. To check this hypothesis molecular modeling studies were performed using the already developed concept<sup>10</sup> using alcuronium as a template. Since all hexamethonium compounds proved to be highly flexible,<sup>10</sup> no systematic search for a global minimum energy conformation was performed. The matching procedure onto alcuronium revealed rather good fits for all diastereomers of **12** using both aromatic rings, either the phthalimidine or the benzylidene (representatively shown for **12a** in Figure 3). The rms (root mean square) values calculated for six atoms are less than 1 and the energy of the conformations is similar in either case. It is tempting to speculate that both conformations of each isomer can be accommodated in the receptor protein, which is an indication of a sort of multiple binding mode phenomenon.<sup>32</sup>

a)



b)

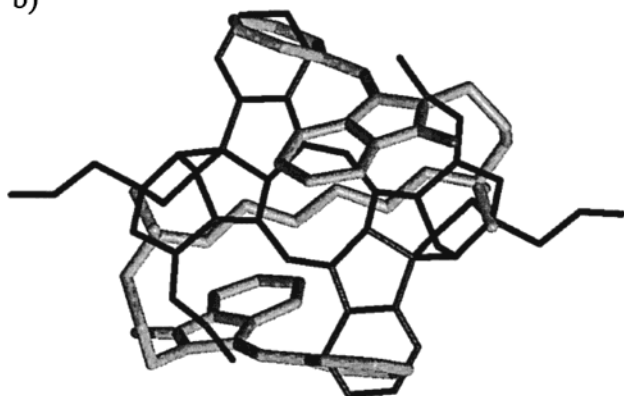


**Figure 3.** Alignment of **12(EE)** onto alcuronium using the positively charged nitrogens and the two aromatic carbon atoms at alcuronium and the phthalimidine moiety (a) or the benzylidene ring (b).

Herein, the ligand uses the same points of attachment of the receptor protein, but different moieties of the ligands are involved.

The fact that the geometric isomers of **12** exhibit the same allosteric potency might be due to the above-described flexibility of the hexamethonium middle chain, which enables the molecule to drive the pharmacophoric elements in the right position upon binding to the receptor protein. By analogy, it might be concluded that the optical isomers of **5**, **9**, and **15** would also exhibit the same allosteric potency. However, the potency is low and it was, thus, not worthwhile to separate the isomers.

### Conclusion

Summing up, electrostatic, van der Waals, and hydrophobic interactions are crucial for receptor recognition. The two positive charges in the middle of the molecules are likely to be responsible for approaching the receptor because they form long-range ion-ion interactions. Substituents of the lateral phthalimido rings in position 3 sensitively influence the allosteric potency, indicating an additional point of interaction. This was shown with benzylidene-substituted compounds. These compounds are much more potent than previously known allosteric modulators. Rigidity, resulting in a smaller loss of conformational entropy upon binding to the receptor protein, polarizability, offering the possibility of dispersive van der Waals interactions,

**Table 4.** Reaction and Physical Data of Compounds **2**, **5a–e**, **9**, **12a–c**, and **15**

compd	mmol	solvent	reaction time (h)	temp (°C)	yield (%)	mp (°C)
<b>2</b>	0.5	HOAc propionic acid	4	reflux	45	246
<b>5a</b>	22	acetone	0.5	reflux	35	162–65
<b>5b</b>	3.5	ethanol	24	reflux	22	83
<b>5c</b>	2.0	acetone	18	reflux	28	60
<b>5d</b>	3.2	MeCN	5.0	reflux	53	130
<b>5e</b>	1.4	i-propanethiol	2.5	reflux	60	148–54
<b>9</b>	1.1	MeCN	72	rt <sup>a</sup>	40	212–15
<b>12b</b>	2.0	MeCN	4–5	80	57	234
<b>12a</b>	3.2	MeCN	4–5	80	64	223
<b>12c</b>	0.17	MeCN	72	rt <sup>a</sup>	52	230
<b>15</b>	1.8	MeCN	4–5	80	54	255

<sup>a</sup> rt = room temperature.

and hydrophobic interactions were deemed important for ligand-receptor interaction. Thus, annellation of further aryl rings to either the imide or the benzylidene moiety should increase the potency. Corresponding investigations are planned.

Since no stereoselectivity concerning the substituent in position 3 could be detected, the allosteric site at the receptor is supposed to be rather large and is likely to be located at the entrance of the ligand binding pocket of the muscarinic receptor protein.

### Experimental Section

Melting points were determined with a Dr. Tottoli point apparatus (Büchi) and were not corrected. <sup>1</sup>H and <sup>13</sup>C NMR spectra were recorded on Varian XL 300 (<sup>1</sup>H NMR, 299.956 MHz; <sup>13</sup>C NMR, 75 MHz) spectrometers. The centers of the peaks of CDCl<sub>3</sub> and DMSO-*d*<sub>6</sub> were used as internal references. Abbreviations for data quoted are d, doublet; t, triplet; q, quartet; quin, quintet; and m, multiplet. Coupling constants are given in hertz. IR spectra, recorded as KBr disks, were obtained using a Perkin-Elmer 298 spectrometer. Dry solvents were used throughout. Chemicals were of analytical grade and purchased from Aldrich, Steinheim, or Merck, (Darmstadt, FRG). Drugs: [<sup>3</sup>H]NMS was purchased from NEN-Dupont (Bad Homburg, FRG). The other drugs, atropine sulfate and (–)-scopolamine methylbromide, were obtained from Sigma Chemicals (München, FRG). The analytical results of the compounds are within ±0.4% of the theoretical values.

**Chemistry.** **2**-{3-[1-(6-{1,1-Dimethyl-1-[3-(1-oxo-2,3-dihydro-1*H*-2-isoindolyl)propyl]ammonio}hexyl)-1,1-dimethylammonio]propyl]-1-isoindolinone Dibromide (**2**). W84 (0.35 g, 0.5 mmol) and Zn powder (1.8 g, 27.6 mmol) were suspended in 25 mL of glacial acid and 2.5 mL of propionic acid. The mixture was refluxed for 4 h and hot and cold filtered, and the filtrate was evaporated to dryness under reduced pressure at 60 °C. The obtained oil was crystallized and recrystallized from ethanol. For analytical and spectroscopic data, see Tables 4 and 5.

***N*-(3-Bromopropyl)-3-hydroxy-1-isoindolinone (3).** Solid sodium borohydride (0.7 g, 18.5 mmol) was carefully added to a solution of *N*-(3-bromopropyl)phthalimide (10.0 g, 37.3 mmol) in dried methanol under cooling. The solution was allowed stand at room temperature for 1 h. Afterward water was added and the resulting mixture was extracted with methylene chloride. The organic layer was dried over Na<sub>2</sub>SO<sub>4</sub> and evaporated in vacuo. The oil was crystallized from ethanol/benzene to give 33% **3**, mp 94 °C.

**General Procedure for the Synthesis of *N*-(3-Bromopropyl)-3-methoxy-1-isoindolinone (4b), *N*-(3-Bromopropyl)-3-ethoxy-1-isoindolinone (4c), and *N*-(3-Bromopropyl)-3-isopropoxy-1-isoindolinone (4d).** A mixture of *N*-(3-bromopropyl)-3-hydroxy-1-isoindolinone (3.62 g, 13.4 mmol), *p*-toluenesulfonic acid (0.22 g, 1.3 mmol), and the corresponding alcohol (26 mmol) was heated under reflux for



Table 5. <sup>1</sup>H NMR Spectroscopic Data of Compounds **2**, **5a–e**, **9**, **15**, and **12a–c** (300 MHz, DMSO-*d*<sub>6</sub>, δ(ppm))

	-C <sup>1</sup> H-N <sup>Phth</sup>	-C <sup>2</sup> H <sub>6</sub> H <sub>b</sub> -	-C <sup>1</sup> H-N <sup>Phth</sup> -C <sup>2</sup> H <sub>6</sub> H <sub>b</sub> -C <sup>3</sup> H <sub>2</sub> -C <sup>4</sup> H <sub>2</sub> -C <sup>5</sup> H <sub>2</sub> -N-C <sup>6</sup> H <sub>2</sub> -C <sup>7</sup> H <sub>2</sub> -	-C <sup>4</sup> H <sub>2</sub> -N-C <sup>5</sup> H <sub>2</sub> -	-C <sup>6</sup> H <sub>2</sub> -	-C <sup>7</sup> H <sub>2</sub> -	+N(CH <sub>3</sub> ) <sub>2</sub>	aromatic	others
<b>2</b>	4.54 (s)-CH <sub>2</sub> -	3.61 (t, 6.3)	2.07 (m)	3.31(m)/3.24(m)	1.64	1.27	3.02 (s)	7.47-7.72 (m)	
<b>5a</b>	5.91 (d)	3.57 (m), 3.50 (m)	2.08 (m)	3.24-3.30/3.48	1.65(m)	1.28 (m)	3.03 (s)	7.49-7.69 (m)	6.65 (d)
<b>5b</b>	6.10 (s)	3.69 (quin), 3.17-3.43 (m)	2.07 (m)	3.17-3.43 (m)	1.66 (m)	1.29 (m)	3.04 (s)	7.56-7.75 (m)	2.94 (s)
<b>5c</b>	6.08 (s)	3.68 (quin), 3.08-3.44 (m)	2.07 (m)	3.08-3.44 (m)	1.66 (m)	1.29 (m)	3.05 (s)	7.54-7.76 (m)	1.10 (t, 7.1), 3.08-3.44 (m)
<b>5d<sup>a</sup></b>	5.99 (s)	3.48-3.78 (m), 3.48-3.78 (m)	2.26 (m)	3.48-3.78 (m)	1.86 (m)	1.46 (m)	3.33 (s)	7.41-7.61 (m), 7.68 (d)	1.17 (d, 6.1), 1.22 (d, 6.61), 3.91 (quin)
<b>5e</b>	6.14 (s)	3.84 (quin), 3.20-3.51 (m)	2.04 (m), 2.14 (m)	3.20-3.51 (m)	1.65 (m)	1.28 (m)	3.04 (s)	7.51-7.75 (m)	0.88 (d, 6.6), 1.06 (d, 6.6), 2.36 (quin)
<b>9<sup>a</sup></b>	5.85 (s)	3.74 (m), 3.32 (m)	2.03 (m)	3.32-3.57 (m)	1.75 (m)	1.38 (m)	3.20 (s)	7.09-7.15 (m), 7.18-7.23 (m), 7.25-7.33 (m), 7.34-7.45 (m), 7.73 (d)	
<b>12a (E)</b>		3.96 (t, 7.1)	2.13 (m)	3.44-3.52 (m), 3.27-3.35 (m)	1.67 (m)	1.26 (m)	3.07 (s)	7.26 (d, 7.5, 2H), 7.37-7.53 (m), 14H), 7.76 (d, 7.5, 2H)	6.98 (s)
<b>12b (Z)</b>		3.63 (t, 7.1)	1.51 (m)	2.76-2.86 (m), 3.05-3.15 (m)	1.51 (m)	1.21 (m)	2.86 (s)	7.36-7.50 (m, 10H), 7.58 (t, 8.0, 2H), 7.69-7.79 (m, 4H), 8.11 (d, 8.0, 2H)	7.16 (s)
<b>12c (Z/E)</b>		3.63 (t, 7.1), 3.96 (t, 7.1)	1.51 (m), 2.13 (m)	2.74-2.86 (m), 3.44-3.50 (m), 3.03-3.14 (m), 3.23-3.36 (m)	1.51 (m), 1.65 (m)	1.22 (m)	2.84 (s), 3.07 (s)	7.26 (d, 7.7, 2H), 7.38-7.62 (m, 10H), 7.69-7.79 (m, 4H), 8.11 (d, 8.0, 2H)	6.95 (s), 7.16 (s)
<b>15</b>	5.12 dd	3.88 (quin)	2.02 (m), 2.14 (m) (AB)	3.28-3.56 (m)	1.67 (m)	1.29 (m)	3.05 (s)	6.99-7.07 (m), 7.12-7.19 (m), 7.29 (d), 7.38-7.58 (m)	3.05-3.15, 3.28-3.56 (m)

<sup>a</sup> In CDCl<sub>3</sub>.

8 h. After evaporation of the excess of alcohol in vacuo, water was added to the residue. The obtained mixture was basified with NaHCO<sub>3</sub> to pH 8 and extracted three times with methylene chloride. The organic layer was washed with water, dried over Na<sub>2</sub>SO<sub>4</sub>, and evaporated in vacuo. The obtained oil was purified by the means of column chromatography (silica gel; mobile phase, hexane/ethyl acetate/methanol = 10:4:1). The residue was recrystallized from methylene chloride/hexane = 1:1) to give 45–60% pure **4b–d**, mp (**4b**) 98 °C, mp (**4d**) 63 °C.

**General Procedure for the Synthesis of 3-Hydroxy-2-{3-[1-(6-{1,1-dimethyl-1-[3-(3-hydroxy-1-oxo-2,3-dihydro-1H-2-isoindolyl)propyl]ammonio}hexyl)-1,1-dimethylammonio]propyl}-1-isoindolinone Dibromide (**5a**), 3-Methoxy-2-{3-[1-(6-{1,1-dimethyl-1-[3-(3-methoxy-1-oxo-2,3-dihydro-1H-2-isoindolyl)propyl]ammonio}hexyl)-1,1-dimethylammonio]propyl}-1-isoindolinone Dibromide (**5b**), 3-Ethoxy-2-{3-[1-(6-{1,1-dimethyl-1-[3-(3-ethoxy-1-oxo-2,3-dihydro-1H-2-isoindolyl)propyl]ammonio}hexyl)-1,1-dimethylammonio]propyl}-1-isoindolinone Dibromide (**5c**), 3-Isopropoxy-2-{3-[1-(6-{1,1-dimethyl-1-[3-(3-isopropoxy-1-oxo-2,3-dihydro-1H-2-isoindolyl)propyl]ammonio}hexyl)-1,1-dimethylammonio]propyl}-1-isoindolinone Dibromide (**5d**) and 3-Phenyl-2-{3-[1-(6-{1,1-dimethyl-1-[3-(3-phenyl-1-oxo-2,3-dihydro-1H-2-isoindolyl)propyl]ammonio}hexyl)-1,1-dimethylammonio]propyl}-1-isoindolinone Dibromide (**9**).** Bis(dimethylamino)hexane was refluxed with phthalimidine derivatives **3**, **4b–d**, and **8** in a polar solvent (see Table 4). The solvent was removed in vacuo. The obtained oil was dissolved in 2 mL of ethanol. After addition of diethyl ether again an oil was obtained and the solvent removed. This procedure was repeated until the phthalimidine derivatives (**3**, **4b–d**, **8**) were completely removed from the residue. The obtained solid residue was recrystallized from a mixture of ethanol/methylene chloride/diethyl ether. For analytical and spectroscopic data, see Tables 4 and 5.

**Synthesis of 3-Isopropylthio-2-{3-[1-(6-{1,1-dimethyl-1-[3-(3-isopropylthio-1-oxo-2,3-dihydro-1H-2-isoindolyl)propyl]ammonio}hexyl)-1,1-dimethylammonio]propyl}-1-isoindolinone Dibromide (**5e**).** **5a** (1.0 g, 1.4 mmol) was dissolved in 2-propanethiol (3.0 g, 39.5 mmol). To the solution were added 5 drops of concentrated hydrochloric acid. Subsequently, the reaction mixture was refluxed for 3 h. The obtained oil was separated from the solution and washed with ethyl acetate. The oil was dissolved in ethanol. After addition of diethyl ether again an oil was obtained, which was washed with ethyl acetate and crystallized from ethanol/ethyl acetate. For analytical and spectroscopic data, see Tables 4 and 5.

**4-Phenyl-1-phthalazone (**6**).** A solution of hydrazine sulfate (4.0 g, 30.4 mmol) and sodium hydroxide (2.4 g, 60.8 mmol) in 20 mL of water was heated on a steam bath for 20 min. The hot solution was added to a hot aqueous solution of benzoylbenzoic acid (6.9 g, 30.4 mmol). The reaction mixture was heated under reflux for 1 h. After cooling and addition of hydrochloric acid, the residue obtained was filtered and washed with water. The crystalline solid was recrystallized from ethanol to give 5.1 g (76%) of **6**: *M*<sub>w</sub> = 222.3, mp 212 °C; <sup>1</sup>H NMR (60 MHz, DMSO-*d*<sub>6</sub>) δ 7.23–8.53 (m, 9H, arom), 16.43 ppm (s, 1H, -NH).

**3-Phenyl-1-isoindolinone (**7**).** To a mixture of phenylphthalazone (4.0 g, 18 mmol), Zn powder (17.6 g, 270 mmol), and 10 mL of water was added 40 mL of concentrated hydrochloric acid carefully. The reaction mixture was heated under reflux for 1 h. To the cooled solution was added water. The mixture was extracted with methylene chloride. The organic layer was dried over Na<sub>2</sub>SO<sub>4</sub> and evaporated in vacuo. The residue was purified by the means of column chromatography (silica gel; mobile phase, benzene/ethyl acetate/methanol = 9:4:1; *R*<sub>f</sub> = 0.4). The crystalline solid was recrystallized from ethanol to give 1.7 g (49%) of **7**: *M*<sub>w</sub> = 209.2, mp 218 °C; <sup>1</sup>H NMR (60 MHz, DMSO-*d*<sub>6</sub>) δ 5.73 (s, 1H, -NCH-), 7.18–7.90 (m, 9H, arom), 9.10 ppm (s, 1H, -NH).

**N-(3-Bromopropyl)-3-phenyl-1-isoindolinone (**8**).** To a solution of 3-phenyl-1-isoindolinone (2.0 g, 9.6 mmol) in 50 mL



of dried THF was added an equimolar amount of sodium hydride. The mixture was heated under reflux for 2 h. 1,3-Dibromopropane (5.8 g, 28.8 mmol) was added and the solution was heated under reflux for additional 5 h. After THF and the excess 1,3-dibromopropane were removed under reduced pressure, the residue was purified by means of column chromatography (silica gel; mobile phase, benzene/ethanol/methanol = 9:4:1;  $R_f$  = 0.51). The crystalline residue was recrystallized from ethanol in 26% yield; mp 106 °C.

**3-Benzaldehyde (10).** A mixture of phthalic anhydride (10.0 g, 67.5 mmol), phenylacetic acid (11.0 g, 81 mmol), and sodium acetate (2.76 g, 33.7 mmol, dry) was heated for 3–4 h up to 250–300 °C. After cooling to room temperature, the solid reaction mixture was crystallized from ethanol to give 10 g (70%) of the *Z* isomer of 3-benzaldehyde:  $M_w$  = 222.2, mp 98–100 °C;  $^1\text{H}$  NMR (60 MHz, DMSO- $d_6$ )  $\delta$  6.40 (s, 1H), 7.16–8.06 ppm (m, 9H, arom).

**3-(*E/Z*)-Benzylidene-*N*-[3-(*N,N*-dimethylamino)propyl]-1-isoindolinone (11 (*E*) and 11 (*Z*)).** A solution of 3-benzaldehyde (6.0 g, 27.0 mmol) and *N,N*-dimethylaminopropylamine (2.8 g, 27.0 mmol) in 10 mL ethanol was refluxed for 4 h. After evaporation of ethanol in vacuo, 50 mL of water was added to the residue. The obtained mixture was extracted with methylene chloride. The organic layer was dried over  $\text{Na}_2\text{SO}_4$  and evaporated in vacuo. The residue was crystallized from diethyl ether to give *N*-[3-(*N,N*-dimethylamino)propyl]-3-hydroxy-3-benzyl-1-isoindolinone. The benzylidene-phthalimidine derivative **11** was obtained after dehydration with formic acid (3 g). The mixture was heated at 130–140 °C for 30 min. After cooling, water was added. The resulting mixture was basified with  $\text{NaHCO}_3$  and extracted with methylene chloride. The organic layer was washed with water, dried over  $\text{Na}_2\text{SO}_4$ , and evaporated. The obtained product **11** is a mixture of about 90% *E* and 10% *Z* isomers. The diastereomers were separated by means of column chromatography on silica gel (mobile phase, methylene chloride/methanol = 5:1;  $R_f(\text{Z})$  = 0.57,  $R_f(\text{E})$  = 0.51).

**3-(*E*)-Benzylidene-*N*-[3-[1-(6-{1-bromoethyl})-1,1-dimethylammonio]propyl]-1-isoindolinone Bromide (13).** A mixture of *N*-[3-(*N,N*-dimethylamino)propyl]-3-(*E*)-benzylidene-phthalimidine (0.54 g, 1.765 mmol) and 1,6-dibromohexane (6.7 g, 27.6 mmol) in 15 mL of acetonitrile was stirred at room temperature for 72 h. Acetonitrile was removed in vacuo. The obtained oil was dissolved in 4 mL of methylene chloride. After addition of diethyl ether again an oil was obtained and the solvent removed. This procedure was repeated until the bisammonium compound (**12a**) was completely removed from the residue (TLC control; eluent, methanol/concentrated  $\text{NH}_3$  = 4.5:1.5;  $R_f(\text{13})$  = 0.133,  $R_f(\text{12a})$  = 0.00). The obtained solid residue was recrystallized from methylene chloride/ethyl acetate to give 0.5 g (52%) of **13**:  $M_w$  = 470, mp 150 °C;  $^1\text{H}$  NMR (300 MHz,  $\text{CDCl}_3$ ,  $\delta$  (ppm)) 7.74 (td, 7.5, 0.9, 1H–arom), 7.25–7.50 (m, 8H–arom), 6.89 (s,  $-\text{C}=\text{CH}$ ), 4.03 (t, 6.5,  $\text{O}=\text{CNCH}_2-$ ), 3.69 (m,  $\text{O}=\text{CNCH}_2\text{CH}_2\text{CH}_2\text{N}^+$ ), 3.54 (m,  $^+\text{NCH}_2-$ ), 3.34 (s,  $^+\text{N}(\text{CH}_3)_2$ ), 3.30 (m, 6.7,  $-\text{CH}_2\text{Br}$ ), 2.29 (m,  $\text{O}=\text{CNCH}_2\text{CH}_2-$ ), 1.75 (m,  $-\text{CH}_2\text{CH}_2\text{Br}$ ), 1.66 (m,  $^+\text{NCH}_2\text{CH}_2-$ ), 1.36 (m,  $^+\text{NCH}_2\text{CH}_2\text{CH}_2\text{CH}_2-$ );  $^{13}\text{C}$  NMR ( $\text{CDCl}_3$ ,  $\delta$  (ppm)) 166.67 ( $-\text{C}=\text{O}$ ), 135.02 (C–arom), 134.81 (C–arom), 134.52 (C–arom), 131.72 (CH–arom), 129.54 (CH–arom), 129.39 (C–arom), 129.39 (CH–arom), 129.25 (CH–arom), 128.48 (CH–arom), 127.84 (CH–arom), 123.18 (CH–arom), 122.88 (CH–arom), 111.82 ( $-\text{C}=\text{CH}-$ ), 64.19 ( $^+\text{NCH}_2-$ ), 61.37 ( $\text{O}=\text{CNCH}_2\text{CH}_2\text{CH}_2\text{N}^+$ ), 51.39 ( $^+\text{N}(\text{CH}_3)_2$ ), 36.46 ( $\text{O}=\text{CNCH}_2-$ ), 33.59 ( $-\text{CH}_2\text{Br}$ ), 32.15 ( $-\text{CH}_2\text{CH}_2\text{Br}$ ), 27.54 ( $^+\text{NCH}_2\text{CH}_2\text{CH}_2-$ ), 25.34 ( $^+\text{NCH}_2\text{CH}_2\text{CH}_2\text{CH}_2-$ ), 22.61 ( $\text{O}=\text{CNCH}_2\text{CH}_2-$ ), 22.48 ( $^+\text{NCH}_2\text{CH}_2-$ ).

**3-Benzyl-2-[3-(*N,N*-dimethylamino)propyl]-1-isoindolinone (14).** A mixture of diastereomers of **11** (1.3 g, 4.2 mmol), 10% Pd/C (300 mg), 300 mL of ethanol, and hydrogen was shaken under 4.4 bar pressure at room temperature for 16 h. After removal of the catalyst by filtration, solvent was removed in vacuo. The product was purified by means of column chromatography (silica gel; mobile phase, methylene chloride/methanol = 5:1) to give 82% of **14**, mp 147–150 °C.

**General Procedure for the Synthesis of 3-(*E*)-Benzylidene-2-[3-[1-(6-{1,1-dimethyl-1-[3-(*E*)-benzylidene-1-oxo-2,3-dihydro-1*H*-2-isoindolyl]propyl]ammonio]hexyl)-1,1-dimethylammonio]propyl]-1-isoindolinone Dibromide (12a), 3-(*Z*)-Benzylidene-2-[3-[1-(6-{1,1-dimethyl-1-[3-(*Z*)-benzylidene-1-oxo-2,3-dihydro-1*H*-2-isoindolyl]propyl]ammonio]hexyl)-1,1-dimethylammonio]propyl]-1-isoindolinone Dibromide (12b), and 3-Benzyl-2-[3-[1-(6-{1,1-dimethyl-1-[3-(3-benzyl-1-oxo-2,3-dihydro-1*H*-2-isoindolyl)propyl]ammonio}hexyl)-1,1-dimethylammonio]propyl]-1-isoindolinone Dibromide (15).** According to the general procedure for the syntheses of **5a–d**, the reaction of 1,6-dibromohexane with the phthalimide derivatives **14** and **11-(*E/Z*)**, respectively, for 5–24 h in a polar solvent, gave **15** and **12a,b**. For analytical and spectroscopic data, see Tables 4 and 5.

**Synthesis of 3-[*Z*]-Benzylidene-2-[3-[1-(6-{1,1-dimethyl-1-[3-(*E*)-benzylidene-1-oxo-2,3-dihydro-1*H*-2-isoindolyl]propyl]ammonio]hexyl)-1,1-dimethylammonio]propyl]-1-isoindolinone Dibromide (12c).** Equimolar amounts (1.8 mmol) of **13** and **11b** were refluxed in acetonitrile for 4–5 h. The solvent was removed in vacuo. The obtained solid residue was dissolved in water and extracted five times with diethyl ether. The water was removed in vacuo and the remaining oil dissolved in methylene chloride. **12c** precipitates upon addition of diethyl ether. The precipitate was recrystallized from a mixture of methylene chloride/ethyl acetate. For analytical and spectroscopic data, see Tables 4 and 5.

**Pharmacology.** A homogenate of porcine heart ventricular myocardium was prepared as described previously in more detail.<sup>33</sup> The membranes were stored in 50 mM Tris-HCl pH 7.4 or in distilled water at  $-80$  °C until use. [ $^3\text{H}$ ]NMS (0.15 nM) equilibrium binding was measured in 3 mM  $\text{MgHPO}_4$ , 50 mM Tris, pH 7.3, 37 °C (“Mg,Tris,Cl, $\text{P}_i$ ” buffer) after 2 h. Nonspecific binding was determined in the presence of 1  $\mu\text{M}$  atropine and did not exceed 4% of total binding. Membrane-bound radioactivity was separated by rapid filtration and washed with  $2 \times 5$  mL of ice-cold incubation buffer. Radioactivity on the filters (Schleicher & Schüll, No. 6; Dassel, F.R.G) was determined by liquid scintillation counting. [ $^3\text{H}$ ]NMS binding under control conditions was characterized by  $K_D \approx 0.5$  nM and  $B_{\text{max}} \approx 100$  fmol/mg of protein, respectively.

All test compounds were studied in Mg,Tris,Cl, $\text{P}_i$  buffer for their ability to retard the dissociation of [ $^3\text{H}$ ]NMS from cardiac muscarinic  $\text{M}_2$ -receptors. After incubating radioligand with the membranes for 30 min, [ $^3\text{H}$ ]NMS dissociation was visualized by addition of 1  $\mu\text{M}$  atropine, alone or in the presence of the test compounds. Dissociation proceeded monophasically under control conditions ( $t_{1/2} \approx 2$  min) and in the presence of the test compounds. The dissociation data were analyzed by nonlinear regression analysis applying a monoexponential decay function to determine the apparent dissociation rate constant  $k_{-1}$  of the radioligand. All test compounds retarded [ $^3\text{H}$ ]NMS dissociation concentration-dependently. A plot of the apparent rate constant of dissociation  $k_{-1}$  versus the concentrations of the test compounds provided concentration-effect curves for the retarding action on the dissociation. Curves were fitted to a four-parameter logistic function. To study the sensitivity of the allosteric action of **12a** for the antagonistic action of obidoxime, [ $^3\text{H}$ ]NMS dissociation experiments were carried out in a buffer consisting of 4 mM  $\text{Na}_2\text{HPO}_4$ , 1 mM  $\text{KH}_2\text{PO}_4$ , pH 7.4, 23 °C (“Na,K, $\text{P}_i$ ” buffer; [ $^3\text{H}$ ]NMS binding characteristics,  $K_D \approx 0.1$  nM,  $B_{\text{max}} \approx 100$  fmol/mg protein, dissociation  $t_{1/2}$  control  $\sim 2.5$  min). The data were analyzed as described previously in detail.<sup>34</sup>

**Molecular Modelling. QSAR Analysis.** The lateral varied *N*-methylimides were built up using the model builder in HyperChem 5.1 (Hypercube Inc. Waterloo, ON, Canada, 1997). Geometry optimization was achieved using the MM+ program implemented in HyperChem. By means of ChemPlus (Hypercube Inc.) the following physicochemical properties were calculated: the octanol/water partition coefficient ( $\log P$ ), the steric parameters volume and surface area, as well as polarizability and refractivity, a chameleon parameter comprising both steric bulk and polarizability. The MOPAC polarizabilities

were calculated from the molecular mechanics optimized geometries using the following command line: AM1 EF GNORM=0.1 POLAR. The mean  $\alpha$ -polarizabilities of MOPAC version 6.12 were used. The allosteric potencies ( $EC_{50}$ ) were transformed in the QSAR form  $\log(1/EC_{50})$ . The QSARs (variable selection, regression, and permutation test) were calculated with in-house written Matlab scripts (Matlab 5.3, The MathWorks Inc. 24 Prime Park Way, Natick, MA) which are available on request.

**Pharmacophore Search.** The isomers of compound **12** were built up using model builder in HyperChem 5.1; the so obtained elongated geometries were optimized by means of the force field calculation MM+ program.

**The Fitting Procedure.** Using this starting geometry the atoms to be overlay have been tethered to the cartesian coordinates of the corresponding alcuronium atoms. After geometry optimization, all applied restraints have been removed and den MM+ calculations were repeated. The so-obtained structures were fitted onto alcuronium using the RMS Fit option of HyperChem 5.1. In alcuronium both positively charged nitrogens and aromatic atoms in indole skeletons adjacent to the pyrrolidine ring were used as fitting atoms. In **12**, both positively charged nitrogens, and either in the phthalimidine skeleton an ipso-atom and the corresponding atom in para position or in the benzylidene moiety the ipso-carbon atom and the atom in para position were chosen for fitting and calculation of the rms value.

**Acknowledgment.** Thanks are due to the Deutsche Forschungsgemeinschaft, DFG, and to the Fonds der Chemischen Industrie, FRG, for financial support, to the KAAD for the grant given to M.H.B.C., to an anonymous referee, who greatly improved the presentation of the QSAR results, and to Modest von Korff for valuable discussions, as well as to Ilona Knoblauch, Iris Witten, and Frauke Mörschel for skillful technical assistance.

**Supporting Information Available:** Spectra (IR and  $^1H$  and  $^{13}C$  NMR) of the intermediates and final products as well as the conformational energy and rms values of the different fit conformations of the isomers of **12** are available free of charge via the Internet at <http://pubs.acs.org>.

## References

- Holzgrabe, U.; Mohr, K. Allosteric modulators of ligand binding to muscarinic acetylcholine receptors. *Drug Discovery Today* **1998**, *3*, 214–222.
- Christopoulos, A.; Lanzafame, A.; Mitchelson, F. Allosteric interactions at muscarinic cholinergic receptors. *Clin. Exp. Pharmacol. Physiol.* **1998**, *25*, 185–19.
- Tränkle, C.; Mohr, K. Divergent modes of action among allosteric modulators of muscarinic  $M_2$  receptors. *Mol. Pharmacol.* **1997**, *51*, 674–682.
- Tränkle, C.; Mies-Klomfass, E.; Botero Cid, M. H.; Holzgrabe, U.; Mohr, K. Identification of a [ $^3H$ ]ligand for the common allosteric site of muscarinic acetylcholine  $M_2$  receptors. *Mol. Pharmacol.* **1998**, *54*, 139–145.
- Proaska, J.; Tucek, S. Mechanism of steric and cooperative actions of alcuronium on cardiac muscarinic acetylcholine receptors. *Mol. Pharmacol.* **1994**, *45*, 709–717.
- Waelbroeck, M.; Robberecht, P.; De-Neef, P.; Christophe, J. Effects of d-tubocurarine on rat muscarinic receptors. *J. Recept. Res.* **1988**, *8*, 787–808.
- Ellis, J.; Seidenberg, M.; Brann, M. R. Use of chimeric muscarinic receptors to investigate epitopes involved in allosteric interactions. *Mol. Pharmacol.* **1993**, *44*, 583–588.
- Jepsen, K.; Lüllmann, H.; Mohr, K.; Pfeffer, J. Allosteric stabilization of  $^3H$ -*N*-methylscopolamine binding in guinea-pig myocardium by an antidote against organophosphorus intoxication. *Pharmacol. Toxicol.* **1988**, *63*, 163–168.
- Holzgrabe, U.; Wagener, M.; Gasteiger, J. Comparison of structurally different allosteric modulators of muscarinic receptors by self-organizing neural networks. *J. Mol. Graph.* **1996**, *14*, 185–193.
- Holzgrabe, U.; Hopfinger, A. J. Conformational analysis, molecular shape comparison, and pharmacophore identification of different allosteric modulators of muscarinic receptors. *J. Chem. Inf. Comput. Sci.* **1996**, *36*, 1018–1024.
- Bejeuhr, G.; Blaschke, G.; Holzgrabe, U.; Mohr, K.; Sürig, U.; Terfloth, G. A stable and highly potent hexamethonium derivative which modulates muscarinic receptors allosterically in guinea-pig hearts. *J. Pharm. Pharmacol.* **1994**, *46*, 108–112.
- Staudt, M.; Tränkle, C.; Mohr, K.; Holzgrabe, U.; Contributions of lateral substituents of heptanebisammonium derivatives to the allosteric modulation of antagonist binding to muscarinic  $M_2$ -receptors. *Life Sci.* **1998**, *62*, 423–429.
- Wassermann, O. Habilitationsschrift, University of Kiel, 1970.
- Dunet, A.; Willemart, A. Produits de reduction du phthalimide; Hydroxyphthalimidine et son. *Bull. Soc. Chem.* **1948**, *189*, 887–889.
- Gabriel, S.; Naumann, A. Über Derivate des Phthalizins und Isoindols. *Ber. Dt. Chem. Ges.* **1893**, *26*, 705–713.
- Gabriel, S. Zur Kenntnis des Benzylidenphthalids. *Ber. Dt. Chem. Ges.* **1885**, *18*, 1251–2433.
- Marsili, A.; Scartoni, V. The structures of 3-benzylidene-phthalide—Primary amine adducts and of *o*-phenylacetylbenzoic acid. *Gazz. Chim. Ital.* **1972**, *102*, 507–516.
- Seydel, J. K.; Schaper, K.-J. *Chemische Struktur und biologische Aktivität*; Verlag Chemie: Weinheim, 1979.
- Kubinyi, H. *QSAR: Hansch Analysis and Related Approaches*; Mannhold, R., Krosggaard-Larsen, P., Timmerman, H., Eds.; VCH: Weinheim, 1993.
- Hansch, C.; Leo, A. *Exploring QSAR—Fundamentals and Applications in Chemistry and Biology*; ACS Professional Reference Book; ACS: Washington, DC 1995.
- Stewart, J. J. P. MOPAC: A semiempirical molecular orbital program. *J. Comput.-Aided Mol. Design*, **1990**, *4*, 1–105.
- Karelson, M.; Lobanov, V. S.; Katritzky, A. R. Quantum-chemical descriptors in QSAR/QSPR studies. *Chem. Rev.* **1996**, *96*, 1027–1043.
- Clerc, J. T.; Terkovic, A. L. Versatile Topological Structure Descriptor for Quantitative Structure/property Studies. *Anal. Chim. Acta* **1990**, *235*, 93–102.
- Baumann, K. Uniform-length molecular descriptors for quantitative structure–property (QSPR), quantitative structure–activity (QSAR), classification studies and similarity searching. *TrAC* **1999**, *18*, 36–46.
- Carhart, R. E.; Smith, D. H.; Venkataraghavan, R. Atom pairs as molecular features in structure–activity studies: Definitions and applications. *J. Chem. Inf. Comput. Sci.* **1985**, *25*, 64–73.
- Kubinyi, H. The Quantitative Analysis of Structure–Activity Relationships. In *Burger's Medicinal Chemistry and Drug Discovery*; Wolff, M. E., Ed.; Wiley: New York, 1995; Vol. 1, part IV, 14, pp 497–572.
- Topliss, J. G.; Edwards, R. P. Chance Factors in Studies of Quantitative Structure–Activity Relationships. *J. Med. Chem.* **1979**, *22*, 1238–1244.
- Wold, S.; Eriksson, L. *Statistical Validation of QSAR Results*, In: *Chemometric Methods in Molecular Design* (van de Waterbeemd, H. Ed.), VCH Verlagsgesellschaft, Weinheim, Germany, 1995, Chapter 5, p 307–318.
- Andrews, P. R. Drug-Receptor Interactions In *3D QSAR in Drug Design—Theory Methods and Applications*; Kubinyi, H., Ed.; ESCOM: Leiden, 1993; pp 13–40.
- Testa, B.; Carrupt, P.-A.; Gaillard, P.; Tsai, R.-S. Intramolecular Interactions Encoded in Lipophilicity: Their Nature and Significance In *Lipophilicity in Drug Action and Toxicology*; Pliska, V., Testa, B., van de Waterbeemd Eds.; VCH Verlagsgesellschaft: Weinheim, Germany, 1996; Chapter 4, pp 48–71.
- Ellis J.; Seidenberg, M. Two allosteric modulators interact at a common site on cardiac muscarinic receptors. *Mol. Pharmacol.* **1992**, *42*, 638–641.
- Kubinyi, H. Lock and Key in the Real World: Concluding Remarks. *Pharm. Acta Helv.* **1994**, *69*, 243–258.
- Tränkle, C.; Kostenis, E.; Burgmer, U.; Mohr, K. Search for lead structures to develop new allosteric modulators of muscarinic receptors. *J. Pharmacol. Exp. Ther.* **1996**, *279*, 926–933.

JM991136E